

Electronic Supplementary Information for

Deciphering the Ultrafast Dynamics of a New Tetraphenylethylene Derivative in Solutions: Charge Separation, Phenyl Rings Rotation and C=C Bond Twisting

Mario de la Hoz Tomás,^a Mao Yamaguchi,^b Boiko Cohen,^{*a} Ichiro Hisaki,^{*b} Abderrazzak Douhal^{*a}

^aDepartamento de Química Física, Facultad de Ciencias Ambientales y Bioquímica, and INAMOL, Universidad de Castilla-La Mancha, Avenida Carlos III, S/N, 45071 Toledo, Spain.

^bGraduate School of Engineering Science, Osaka University, 1-3 Machikaneyama, Toyonaka, Osaka 560-8531, Japan.

Table of Contents

1. General	1
2. Synthesis and characterization of TTECOOBu	3
3. Photophysical properties of TTECOOBu	6
4. Equations for a reversible molecular system	15
5. References	16

1. General

All commercially available reagents and solvents were used without further purification unless otherwise noted. NMR spectra were recorded on a Bruker AV400M (400 MHz) spectrometer. Residual proton and carbon of deuterated solvents were used as internal standards: $\delta = 7.26$ ppm (CDCl_3), for ^1H NMR, $\delta = 77.00$ ppm (CDCl_3) for ^{13}C NMR. HR-MS analysis were performed on a JEOL JMS-700 instrument. ATR-FTIR spectrum of TTECOOBu was recorded at a spectral resolution of 2 cm^{-1} using a JASCO FT/IR-4200 spectrometer.

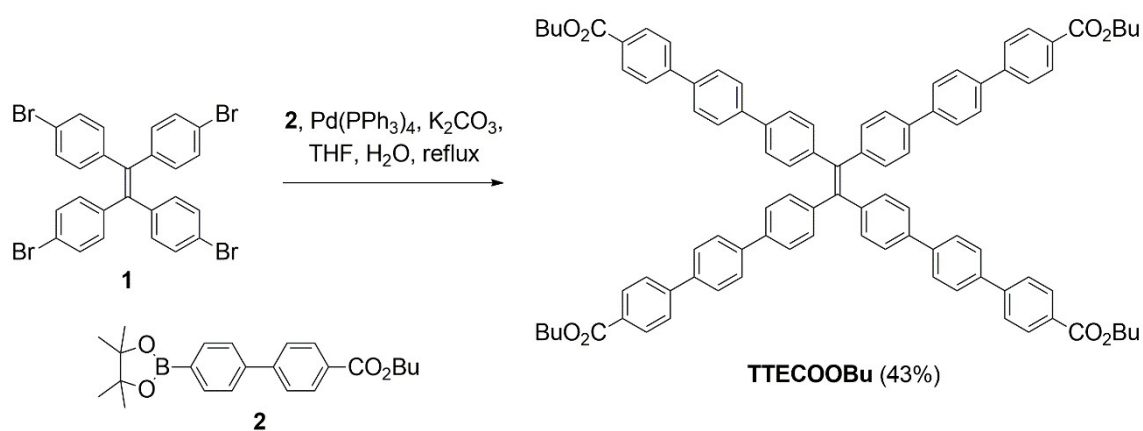
Time-Correlated Single-Photon Counting (TCSPC): The picosecond (ps) time-resolved emission experiments were carried out by employing a time-correlated single-photon counting (TSCPC) system. The samples were excited either by a 40 ps-pulsed (<1 mW, 40 MHz repetition rate) diode-laser (PicoQuant) centred at 371 nm or by 325 nm from the output of a femtosecond (fs) optical parametric oscillator (OPO, Inspire Auto 100, Radiantis), respectively. The fluorescence signal was collected at the magic angle (54.7°) and monitored at a 90° angle to the excitation beam at discrete emission wavelengths.

Fluorescence Up-Conversion: The femtosecond (fs) emission transients were collected using the fluorescence up-conversion technique. Briefly, the system consists of a fs Ti:sapphire oscillator (MaiTai HP, Spectra Physics, 810 nm, 90 fs, 2.75W mW, 80 MHz) coupled to an optical parametric oscillator (OPO, Inspire Auto 100, Radiantis) and up-conversion setups. The OPO output was centered at 650 nm and doubled in an optical setup through a 0.5 mm BBO crystal to generate a pumping beam at 325 nm (~ 0.1 nJ). The polarization of the latter was set to the magic angle with respect to the fundamental 810-nm beam. The sample was placed in a 1 mm thick rotating quartz cell. The fluorescence was focused with reflective optics into a 0.5 mm BBO crystal and gated with the remaining fundamental (810 nm) fs-beam.

Transient Absorption: The fs-transient absorption experiments were realized using a chirped pulse amplification setup that consists of a Ti:Sapphire oscillator (TISSA 50, CDP Systems) pumped by a 5 W diode laser (Verdi 5, Coherent). The seed pulse (30 fs, 450 mW at 86 MHz) centered at 800 nm is directed to a chirped pulse amplification system (Legend-USP, Coherent). The amplified fundamental beam (50 fs, ~ 3.1 W at 1 kHz) is then split by a beam splitter and the main portion (2.7 W) is directed through an optical parametric amplifier for wavelength conversion (TOPAS, Light Conversion). A small portion of the remaining fundamental beam ($\sim 200\ \mu\text{W}$) goes through a delay line

(7.8 fs step and 2 ns of maximum delay) and is focused on a 3-mm thick sapphire crystal for white light continuum (WLC) generation. The produced WLC is split into two parts to form probe and reference beams, which are directed to the sample, where the probe and the pump beams are overlapped. The polarization of the pump is set to the magic angle in respect to the probe. The transmitted light is focused to light guides, directed to a spectrograph, and collected by a pair of photodiode arrays (1024 elements, for spectral measurements). To avoid photo degradation and re-excitation by consecutive pulses, the samples were placed in a 0.8-mm thick rotating quartz cell.

2. Synthesis and characterization of TTECOOBu



TTE-COOBu. A mixture of 1,1,2,2-tetrakis(4-bromophenyl)ethene **1** (600 mg, 0.92 mmol), pinacolate **2** (1.62 mg, 467 μ mol), Pd(PPh₃)₄ (600 mg, 519 μ mol), and K₂CO₃ (2.40 g, 17.3 mmol) in deoxygenated THF (50 mL) and H₂O (15 mL) was stirred at 75 $^{\circ}$ C for 18 h. The organic layer was extracted with CHCl₃, washed with water and brine, dried over anhydrous MgSO₄, and concentrated with a rotary evaporator to afford crude, black solid. The product was purified by column chromatography (silica gel, CHCl₃) and preparative HPLC with gel permeation chromatograph to afford TTECOOBu (531 mg, 0.40 mmol, 43%) as a yellow solid.

M.P. 250 $^{\circ}$ C. ¹H NMR (400 MHz, CDCl₃) δ : 8.12 (d, J = 8.4 Hz, 8H), 7.69 (d, J = 6.4 Hz, 24H), 7.48 (d, J = 8.4 Hz, 8H), 7.28 (d, J = 8.4 Hz, 8H), 4.38 (t, J = 6.8 Hz, 8H), 1.74-1.82 (m, 8H), 1.45-1.53 (m, 8H), 1.00 (t, J = 7.4 Hz, 12H) ppm. ¹³C NMR (100 MHz, CDCl₃) δ : 166.7, 145.0, 143.2, 140.7, 140.4, 139.0, 138.5, 132.2, 130.2, 129.5, 127.7, 127.5, 127.0, 126.5, 65.0, 31.0, 19.4, 13.9 ppm. HR-MS (FAB): Calcd for C₉₄H₈₅O₈ [M+H]⁺ 1340.6166; found: 1340.6154. IR(ATR) 3028.7 (C-H stretching of phenyl groups), 2957.3, 2931.3, 2871.3 (these correspond to C-H stretching of the butyl

group) 1710.6 (ester carbonyl stretching), 1607.4 (alkene bond stretching), 1272.8 cm^{-1} (acyl C=O stretching).

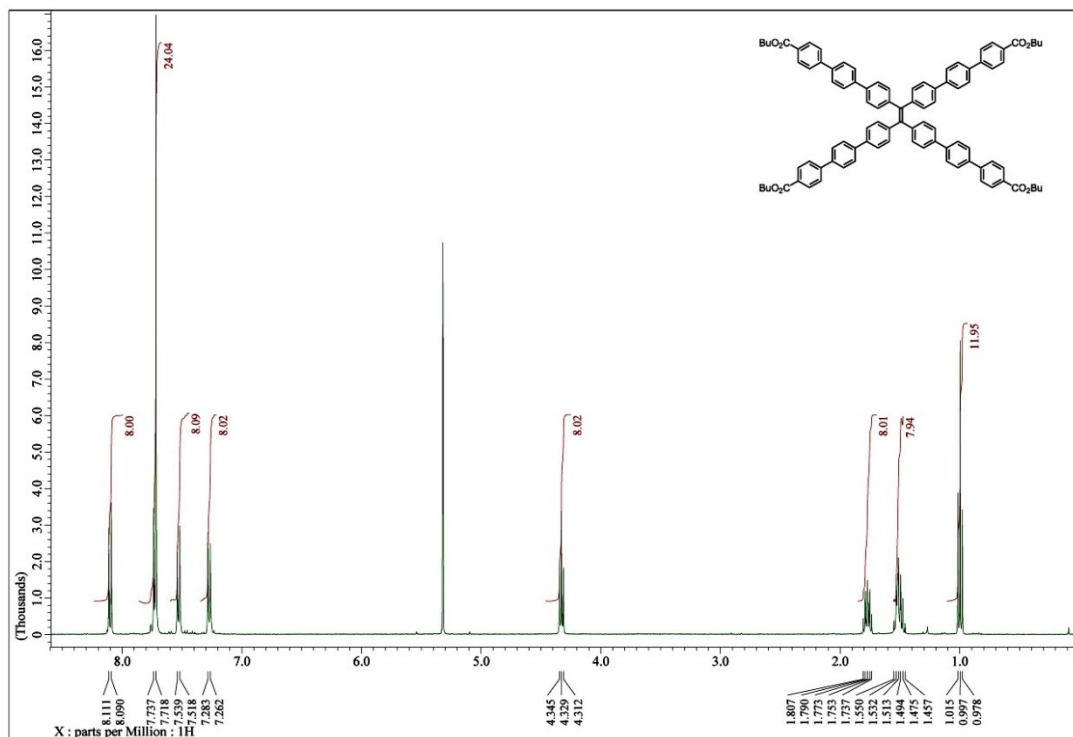


Figure S1. ^1H NMR (400 MHz, CDCl_3) spectrum of TTECOOBu.

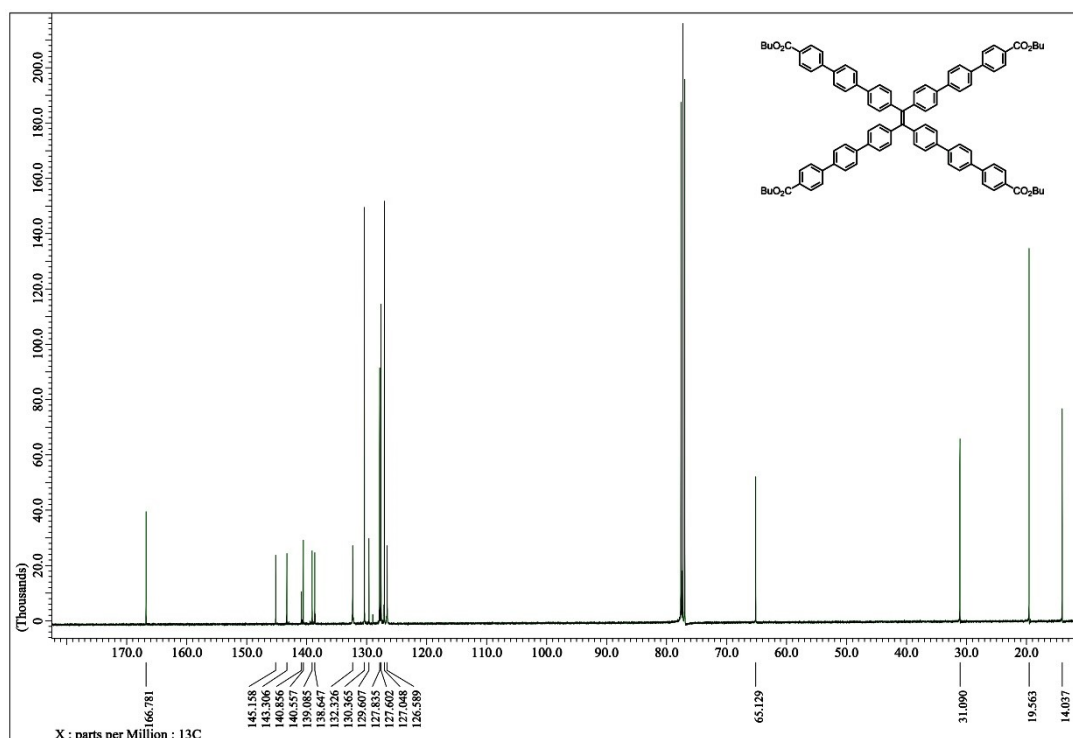
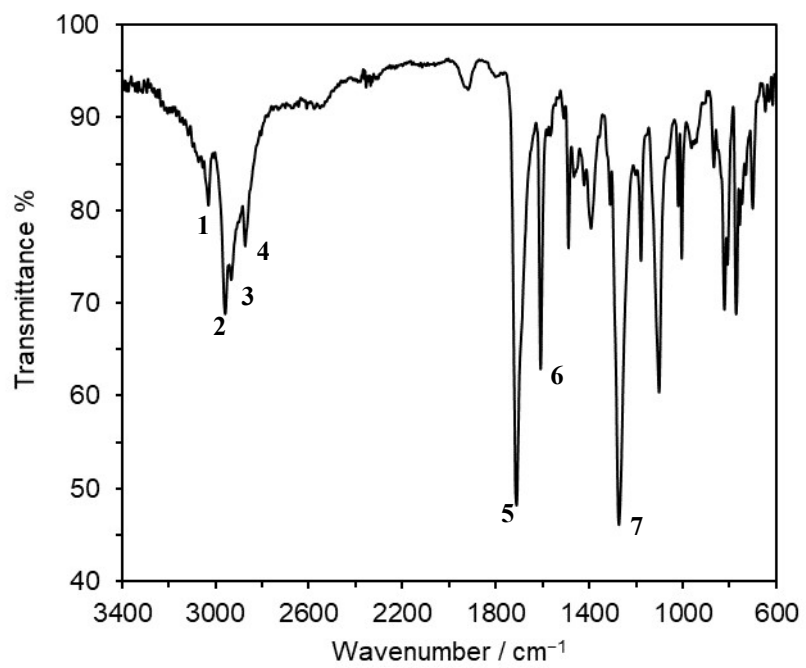


Figure S2. ^{13}C NMR (100 MHz, CDCl_3) spectrum of TTECOOBu.



**Figure
S3.**
ATR-

FTIR spectrum of **TTECOOBu**.

3. Photophysical properties of TTECOOBu

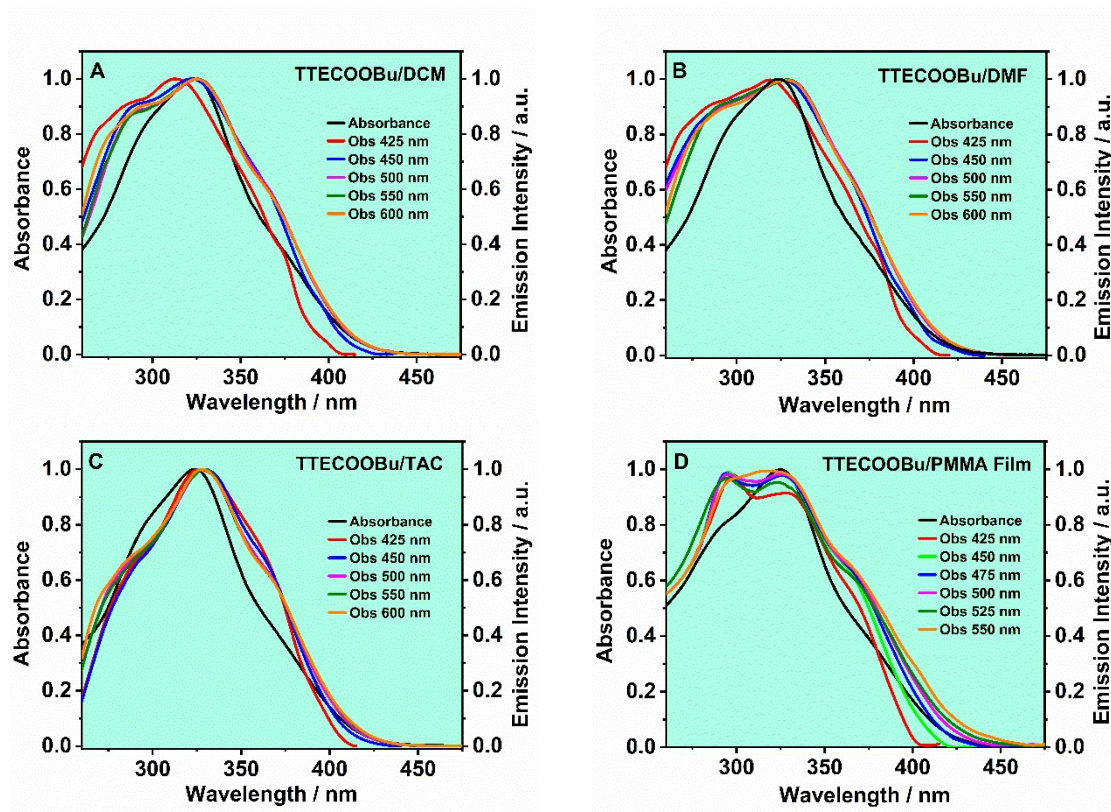


Figure S4. Normalized UV-visible absorption and excitation spectra of TTECOOBu in (A) DCM, (B) DMF, (C) TAC solutions and (D) PMMA film. The observation wavelengths for the excitation spectra are shown in the inset.

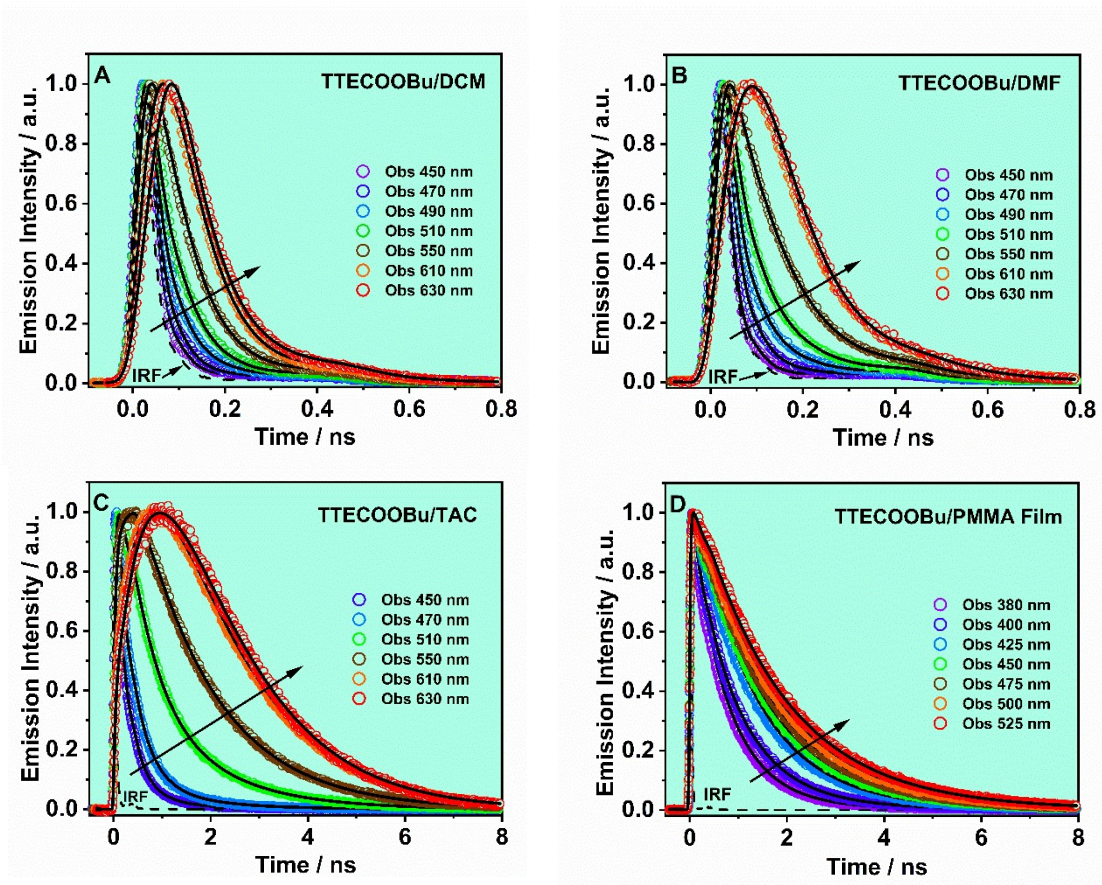


Figure S5. Magic-angle emission decays of TTECOOBu in (A) DCM, (B) DMF, (C) TAC solutions and (D) PMMA film, upon excitation 325 nm and observation as indicated in the inset. The solid lines are from the best multiexponential fits, and the IRF is the instrumental response function.

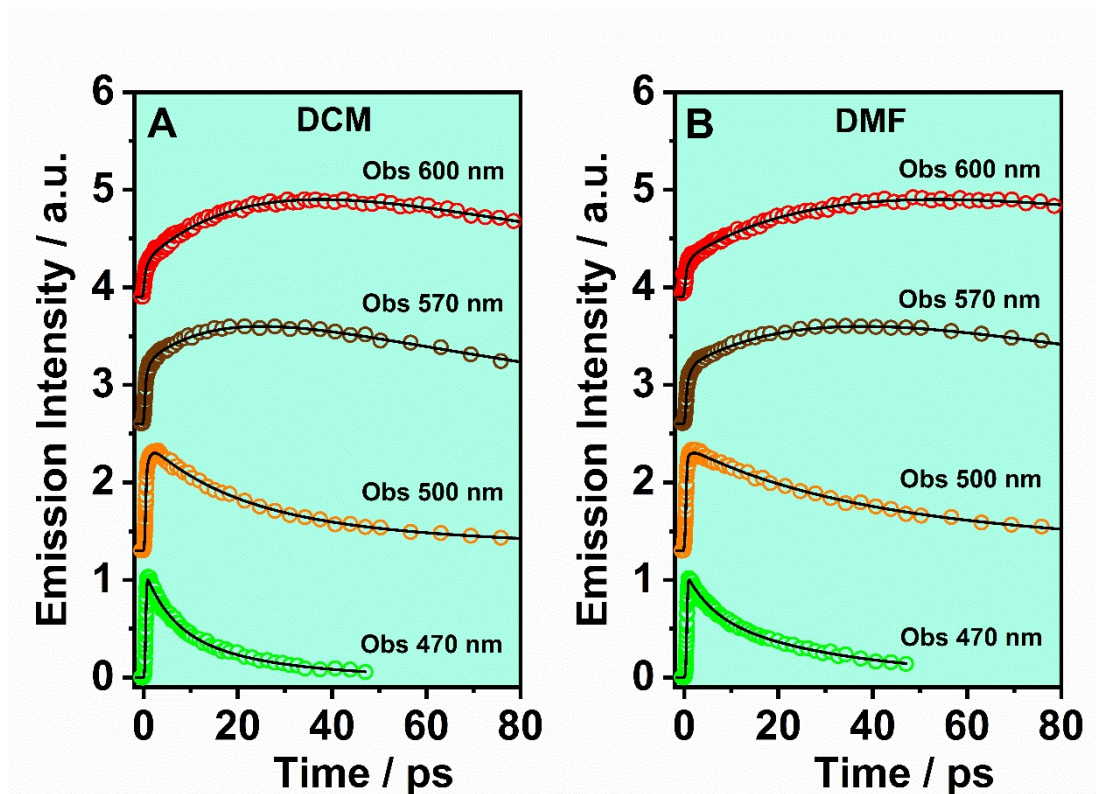


Figure S6. Femtosecond emission transients of TTECOOBu in (A) DCM and (B) DMF solutions. The samples were excited at 325 nm and gated at the indicated wavelengths. The solid lines are from the best multiexponential fit and the IRF is the instrumental response function (~ 320 fs).

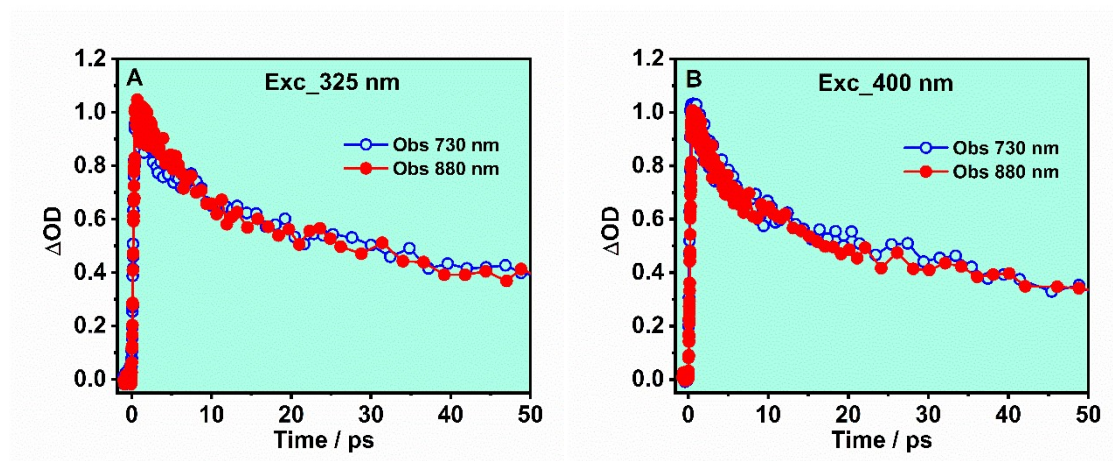


Figure S7. Comparison of representative transient absorption decays of TTECOOBu in a DCM solution, upon excitation at 325 nm (A) and 400 nm (B).

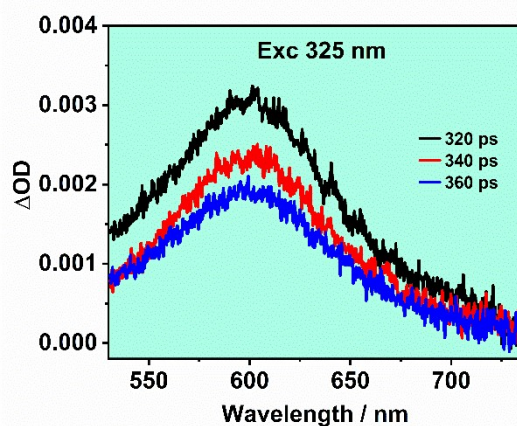


Figure S8. Time-resolved transient absorption spectra of **TTECOOBu** in DCM at longer delay times upon excitation at 325 nm.

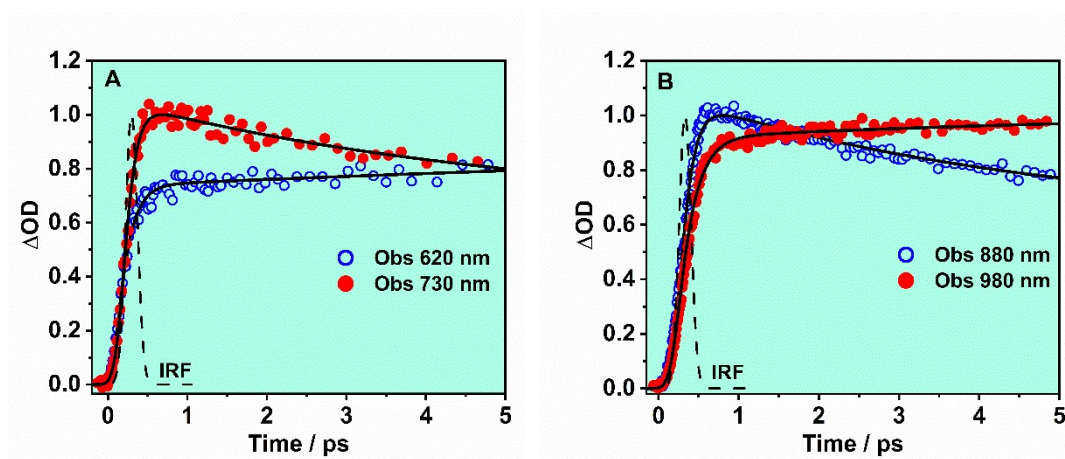


Figure S9. Representative transient absorption decays of **TTECOOBu** in a DCM solution, upon excitation at 325 nm and recorded at visible (A) and NIR (B) region. The solid lines are from the best multiexponential fits, and the IRF is the instrumental response function (~ 100 fs).

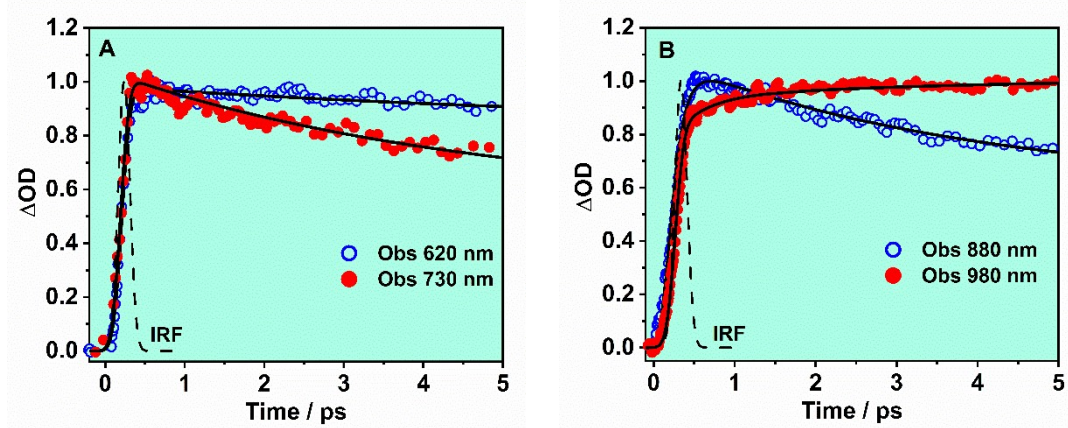


Figure S10. Representative transient absorption decays of TTECOOBu in a DCM solution, upon excitation at 400 nm and recorded at visible (A) and NIR (B) region. The solid lines are from the best multiexponential fits, and the IRF is the instrumental response function (~ 100 fs).

Table S1. Values of time constants (τ_i), amplitudes (A_i), normalized (to 100) pre-exponential factor (a_i) and contribution (c_i) obtained from the fit of the emission ps-ns decays of **TTECOOBu** in a DCM solution, upon excitation at 371 nm and observation as indicated. A negative sign of a_i indicates a rising component in the emission signal. The error in determination of τ_i was within 10 - 15%.

$\lambda_{\text{obs}} / \text{nm}$	τ_1 / ns	A_1	a_1	c_1	τ_2 / ns	A_2	a_2	c_2	τ_3 / ns	A_3	a_3	c_3	A_1/A_2
450	0.03	462	67	17	0.08	172	25	17	1.04	52	8	66	-
480		1726	71	44		681	28	46		11	1	10	-
510		1847	54	31		1574	46	69				-	
540		598	17	7		2919	83	93				-	
570		(-)1255	(-)100	(-)100		3982	100	100				-0.32	
600		(-)2166	(-)100	(-)100		4022	100	100			-	-0.54	
640		(-)3318	(-)100	(-)100		4472	100	100				-0.74	
680		(-)4921	(-)100	(-)100		5039	100	100				-0.98	

Table S2. Values of time constants (τ_i), amplitudes (A_i), normalized (to 100) pre-exponential factor (a_i) and contribution (c_i) obtained from the fit of the emission ps-ns decays of **TTECOOBu** in a DMF solution, upon excitation at 371 nm and observation as indicated. The negative sign of a_i indicates a rising component in the emission signal. The error in determination of τ_i was within 10 - 15%.

$\lambda_{\text{obs}} / \text{nm}$	τ_1 / ns	A_1	a_1	c_1	τ_2 / ns	A_2	a_2	c_2	τ_3 / ns	A_3	a_3	c_3	A_1/A_2
450	0.05	517	72	25	0.10	152	21	15	1.15	54	7	60	-
480		980	69	46		426	30	40		13	1	14	-
510		2089	55	38		1678	45	62				-	
540		161	5	3		3064	95	97				-	
570		(-)2073	(-)100	(-)100		4208	100	100				-0.49	
600		(-)3250	(-)100	(-)100		5217	100	100			-	-0.62	
640		(-)4597	(-)100	(-)100		5923	100	100				-0.78	
680		(-)7191	(-)100	(-)100		7261	100	100				-0.99	

Table S3. Values of time constants (τ_i), amplitudes (A_i), normalized (to 100) pre-exponential factor (a_i) and contribution (c_i) obtained from the fit of the emission ps-ns decays of **TTECOOBu** in a TAC solution, upon excitation at 371 nm and observation as indicated. The negative sign of a_i indicates a rising component in the emission signal. The error in determination of τ_i was within 10 - 15%.

$\lambda_{\text{obs}} / \text{nm}$	τ_1 / ns	A_1	a_1	c_1	τ_2 / ns	A_2	a_2	c_2	τ_3 / ns	A_3	a_3	c_3	A_1/A_2
450		1745	71	44		681	28	48		34	1	8	-
470	0.17	1217	55	26		899	40	53		107	5	21	-
490		606	32	10	0.47	1005	53	45		301	15	45	-
510	0.18	(-)486	(-)100	(-)100		1642	65	36		892	35	64	-
530	0.20	(-)577	(-)100	(-)100		927	44	19	1.55	1164	56	81	-
550	0.20	(-)696	(-)100	(-)100		-	-	-		1907	100	100	-0,36
570	0.45	(-)1276	(-)100	(-)100		-	-	-		2413	100	100	-0,53
590	0.64	(-)2211	(-)100	(-)100		-	-	-		3162	100	100	-0,70
610	0.80	(-)6368	(-)100	(-)100		-	-	-		7723	100	100	-0,82
630	0.95	(-)6587	(-)100	(-)100		-	-	-		7260	100	100	-0,91

Table S4. Values of time constants (τ_i), amplitudes (A_i), normalized (to 100) pre-exponential factor (a_i) and contribution (c_i) obtained from the fit of the emission ps-ns decays of **TTECOOBu** in PMMA Film, upon excitation at 371 nm and observation as indicated. The error in determination of τ_i was within 10 - 15%.

Medium	$\lambda_{\text{obs}} / \text{nm}$	τ_1 / ns	A_1	a_1	c_1	τ_2 / ns	A_2	a_2	c_2
PMMA Film	420		1174	89	82		145	11	18
	450		1068	70	59		457	30	41
	475	1.17	1123	54	43	1.91	956	46	57
	500		743	38	38		1212	62	72
	525		521	29	20		1275	71	80
	550		326	22	15		1155	78	95

Table S5. Values of time constants (τ_i), normalized (to 100) pre-exponential factor (a_i) and contribution (c_i) obtained from the fit of the emission ps-ns decays of **TTECOOBu** in a DCM solution, upon excitation at 325 nm and observation as indicated. A negative sign of a_i indicates a rising component in the emission signal. The error in determination of τ_i was within 10 - 15%.

$\lambda_{\text{obs}} / \text{nm}$	τ_1 / ns	a_1	c_1	τ_2 / ns	a_2	c_2	τ_3 / ns	a_3	c_3
450		84	19		9	7	1.14	7	74
470		76	36		23	38		1	26
490	0.02	96	78	0.07	4	22			
510		77	33		23	67			
530		63	19		37	81			
550		(-100)	(-100)		100	100			
570		(-100)	(-100)		100	100		-	
590	0.04	(-100)	(-100)	0.07	100	100			
610		(-100)	(-100)		100	100			
630		(-100)	(-100)		100	100			

Table S6. Values of time constants (τ_i), normalized (to 100) pre-exponential factor (a_i) and contribution (c_i) obtained from the fit of the emission ps-ns decays of **TTECOOBu** in a DMF solution, upon excitation at 325 nm and observation as indicated. The negative sign of a_i indicates a rising component in the emission signal. The error in determination of τ_i was within 10 - 15%.

$\lambda_{\text{obs}} / \text{nm}$	τ_1 / ns	a_1	c_1	τ_2 / ns	a_2	c_2	τ_3 / ns	a_3	c_3
450		82	22		12	9	1.31	6	69
470		74	32		24	31		2	37
490	0.03	89	48	0.09	11	52			
510		80	31		20	69			
530		60	14		40	86			
550		(-100)	(-100)		100	100			
570		(-100)	(-100)		100	100		-	
590	0.05	(-100)	(-100)	0.09	100	100			
610		(-100)	(-100)		100	100			
630		(-100)	(-100)		100	100			

Table S7. Values of time constants (τ_i), normalized (to 100) pre-exponential factor (a_i) and contribution (c_i) obtained from the fit of the emission ps-ns decays of **TTECOOBu** in a TAC solution, upon excitation at 325 nm and observation as indicated. A negative sign of a_i indicates a rising component in the emission signal. The error in determination of τ_i was within 10 - 15%.

$\lambda_{\text{obs}} / \text{nm}$	τ_1 / ns	a_1	c_1	τ_2 / ns	a_2	c_2	τ_3 / ns	a_3	c_3
450		80	61		18	31		2	8
470	0.23	62	37		33	44		5	19
490		27	10	0.52	56	47		17	43
510	0.13	(-100)	(-100)		63	36		37	64
530	0.21	(-100)	(-100)		41	19	1.55	59	81
550	0.22	(-100)	(-100)		-			100	100
570	0.42	(-100)	(-100)		-			100	100
590	0.59	(-100)	(-100)		-			100	100
610	0.73	(-100)	(-100)		-			100	100
630	0.95	(-100)	(-100)		-			100	100

Table S8. Values of time constants (τ_i), normalized (to 100) pre-exponential factor (a_i) and contribution (c_i) obtained from the fit of the emission ps-ns decays of **TTECOOBu** in PMMA Film, upon excitation at 325 nm and observation as indicated. The error in determination of τ_i was within 10 - 15%.

$\lambda_{\text{obs}} / \text{nm}$	τ_1 / ns	a_1	c_1	τ_2 / ns	a_2	c_2	τ_3 / ns	a_3	c_3
380		40	20		59	80		-	
400	0.40	17	8		74	92		-	
425		-			74	65		26	35
450		-		1.10	44	34		56	66
475		-			23	17		77	83
500		-			2	2	1.90	98	98
525		-			1	1		99	99
550		-			-			100	100
570		-			-			100	100

4. Equations for a reversible molecular system

To analyze the equilibrium state in order to get the values of the involved times of direct and reverse twisting motion, the emission decays were fitted according to the following reactions¹⁻⁶:

$$I_f(CRS) = A_{11}e^{-t/\tau_1} + A_{12}e^{-t/\tau_2} \quad (1)$$

$$I_f(TICT) = A_{21}e^{-t/\tau_1} + A_{22}e^{-t/\tau_2} \quad (2)$$

$$A = A_{12}/A_{11} \quad (3)$$

where τ_1 and τ_2 are the time constants of the fast and slow component respectively, A_{11} , A_{12} and A_{21} , A_{22} are the amplitudes in the bluest (1) and reddest (2) part of emission spectrum. The selected observation wavelengths were: (1) 450 nm (charge resonant structure - CRS) and (2) 680 nm (conformationally twisted species - TICT). The amplitudes at the reddest part of emission spectra are very similar in value but opposite in sign ($A_{r1}/A_{r2} \sim -1$) which is a necessary condition to a reversible reaction.

Using the values of τ_1 , τ_2 together with the amplitude's ratio (A_{12}/A_{11}) at the bluest observation wavelength, and the lifetime of charge resonance structure observed in the bluest part of emission spectra ($\tau_3 = 1.04$ ns and $\tau_3 = 1.15$ ns for DCM and DMF, respectively), the direct and reverse twisting motion constant (k_{DT} and k_{RT}) and the lifetime of conformationally twisted species, τ_{TICT} , were calculated by application of the following equations¹⁻⁶:

$$k_{DT} = \frac{\frac{1}{\tau_1} + \frac{A}{\tau_2}}{1 + A} - \frac{1}{\tau_{CRS}} \quad (4)$$

$$k_{RT} = \frac{\left(\frac{1}{\tau_2} - \frac{1}{\tau_1}\right)^2 - \left(2 \cdot k_{DT} + \frac{2}{\tau_{CRS}} - \frac{1}{\tau_1} - \frac{1}{\tau_2}\right)^2}{4 \cdot k_{DT}} \quad (5)$$

$$\frac{1}{\tau_{TICT}} = \frac{1}{\tau_1} \cdot \left(1 + k_{RT} \cdot \frac{\tau_{CRS} - \tau_1}{1 + k_{DT} \cdot \tau_{CRS} - \frac{\tau_{CRS}}{\tau_1}} \right) \quad (6)$$

5. References

- 1 Y. V. Il'ichev, W. Kühnle and K. A. Zachariasse, *J. Phys. Chem. A*, 1998, **102**, 5670.
- 2 A. Demeter, T. Bérces and K. A. Zachariasse, *J. Phys. Chem. A*, 2001, **105**, 4611.
- 3 K. A. Zachariasse, T. Yoshihara and S. I. Druzhinin, *J. Phys. Chem. A*, 2002, **106**, 6325.
- 4 S. I. Druzhinin, N. P. Ernsting, S. A. Kovalenko, L. P. Lustres, T. A. Senyushkina and K. A. Zachariasse, *J. Phys. Chem. A*, 2006, **110**, 2955.
- 5 M. Gutierrez, N. Alarcos, M. Liras, F. Sánchez and A. Douhal, *J. Phys. Chem. B*, 2015, **119**, 552.
- 6 N. Alarcos, M. Gutiérrez, M. Liras, F. Sánchez, M. Moreno and A. Douhal, *Phys. Chem. Chem. Phys.*, 2015, **17**, 14569.